

Observation of rapid Auger recombination in optically excited semiconducting carbon nanotubes

Feng Wang,¹ Gordana Dukovic,² Ernst Knoesel,^{1,*} Louis E. Brus,² and Tony F. Heinz¹

¹*Departments of Physics and Electrical Engineering, Columbia University, 538 West 120th Street, New York, New York 10027, USA*

²*Department of Chemistry, Columbia University, 3000 Broadway, New York, New York 10027, USA*

(Received 3 September 2004; published 15 December 2004)

Time-resolved fluorescence measurements of single-walled carbon nanotubes (SWNTs) reveal rapid electron-hole pair annihilation when multiple electron-hole pairs are present in a nanotube. The process can be understood as Auger recombination with a rate of $\sim 1 \text{ ps}^{-1}$ for just two electron-hole pairs in a 380-nm long SWNT. This efficient nonradiative recombination reflects the strong carrier-carrier interactions in the quasi-one-dimensional SWNTs. In addition to affecting nanotube fluorescence, Auger recombination imposes limitations on the sustained electron-hole density achievable within a SWNT.

DOI: 10.1103/PhysRevB.70.241403

PACS number(s): 78.47.+p, 78.55.-m, 78.67.Ch, 79.20.Fv

A characteristic feature of one-dimensional (1D) systems is the dramatic enhancement of interaction between charge carriers, an effect arising from their strong spatial confinement and reduced effectiveness in screening. Auger recombination, which involves the annihilation of an electron-hole pair with the released energy transferred to other charge carriers, is representative of an interaction involving multiple carriers. As such, this process, already important in bulk semiconductors, is expected to assume greater prominence in 1D materials. Single-walled carbon nanotubes (SWNTs),¹ with their small diameter and large aspect ratio, provide a model 1D system^{2,3} in which to examine this effect. Such an investigation, in conjunction with previous studies of Auger processes in other material systems, including bulk semiconductors, quantum wells, and nanoparticles, will help us understand the role of dimensionality in carrier-carrier interactions. In addition to this broad fundamental interest, Auger recombination in carbon nanotubes is also a subject of technological relevance. Recent progress in the fabrication of ambipolar nanotube field-effect transistors⁴ and the observation of electroluminescence⁵ from semiconducting nanotubes has sparked interest in using nanotubes in bipolar electronics and as light-emitting devices. In bulk semiconductors and quantum structures, Auger recombination is already well known to play a limiting role in light-emitting^{6,7} and light-harvesting devices,⁸ as well as in power transistors⁹ at high electron-hole densities. Auger recombination has also been shown to strongly affect the carrier dynamics in semiconductor nanoparticles^{10,11} and their properties for light amplification and lasing.¹² In SWNTs, considerable effort has recently been devoted to measurements of carrier dynamics.^{13–16} There has, however, yet to be a clear experimental identification of the Auger effect and a determination of its characteristics in this important and prototypical 1D material system.

In this Rapid Communication, we demonstrate that the Auger effect plays a dominant role in the carrier dynamics of SWNTs when multiple excitations are present. The results are obtained by time-resolved measurements of the fluorescence emission as a function of fluence of an ultrafast laser excitation pulse. The approach permits us to explore the response from the regime of, at most, one electron-hole pair in each nanotube to the regime of multiple excitations. A clear

signature of an Auger process is seen in the emergence of a rapid decay component at elevated excitation densities, combined with unchanged emission at long delay times where, at most, one electron-hole pair remains in any nanotube. From a quantitative analysis of this behavior, we obtain an Auger recombination rate of 0.8 ps^{-1} for two electron-hole pairs in our typical SWNT of $\sim 1 \text{ nm}$ in diameter and $\sim 380 \text{ nm}$ in length. The high Auger rate is a consequence of strong carrier-carrier interactions in SWNTs and appears to limit the sustained electron-hole pair density that can be achieved in these systems.

In our experiments, isolated SWNTs samples were prepared as a micellar suspension in water following a procedure similar to that of O'Connell *et al.*¹⁷ Briefly, bundles of SWNTs grown using the HiPCO approach¹⁸ were dispersed in an aqueous solution of poly(acrylic acid) (PAA, MW $\sim 60\,000$, 1% w/v). The nanotube bundles were separated and purified by sonication and centrifugation at $\sim 110\,000\times g$. This procedure resulted in isolated, fluorescent SWNTs. Atomic force microscopy (AFM) images of 175 nanotubes indicated that most of the nanotubes are 100–500-nm long, with an average length of $\sim 380 \text{ nm}$. From the height of the nanotubes observed in the AFM image, we confirmed that the sample was indeed comprised of individual SWNTs, rather than of bundles. Isolated nanotube samples were also prepared using poly(maleic acid/octyl vinyl ether) as a surfactant. The choice of surfactant had no significant influence on the carrier dynamics reported below.

Measurement of the temporal evolution of the fluorescence from semiconducting SWNTs is achieved through optical pumping with a femtosecond laser and analysis of the fluorescence by optical Kerr gating.^{19,20} The laser source for these measurements is an amplified mode-locked Ti:sapphire system, which delivers pulses of approximately 150 fs duration at a wavelength of 810 nm and a repetition rate of 1 kHz. SWNTs are excited by a portion of the optical pulse. The resulting fluorescence is focused into a 3-mm-thick CS₂ Kerr cell that is placed between a pair of crossed polarizers. The other portion of the optical pulse, which serves as the gate pulse, is directed into the Kerr cell at a suitable delay time. The gated fluorescence is then detected by an InGaAs photodiode.

Experimental fluorescence decay curves for several differ-

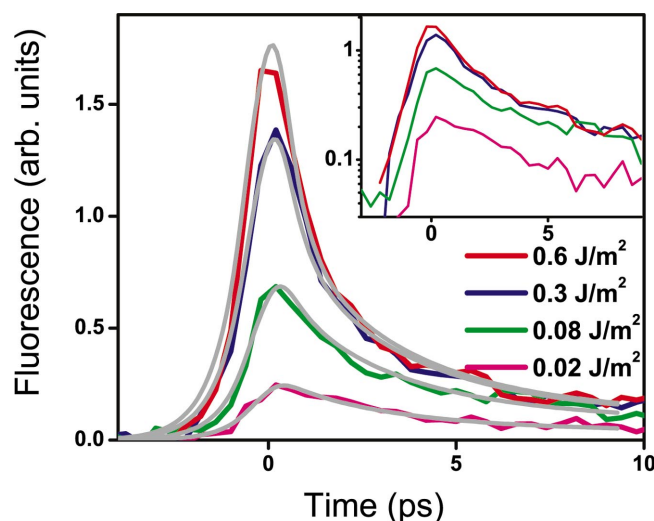


FIG. 1. (Color) Experimental time-resolved fluorescence decay curves for SWNTs excited at the indicated pump fluences. The gray curves are fits using the model described in the text. The inset shows a log-linear plot of the same data. The equivalence of the trailing part of the decay at all fluences is apparent.

ent pump fluences are presented in Fig. 1. The most striking aspect of these curves is the emergence of a fast decay component at high pump fluence, a feature that becomes sharper and more pronounced with increasing excitation density. In contrast, the higher pump fluence has no effect on the temporal evolution of the slow decay component of the fluorescence, which has a time constant of ~ 7 ps associated with defect trapping.²¹ This behavior is most clearly seen in the log-linear representation of the data in the inset of the Fig. 1.

Let us now consider the variation of the amplitude of the emission with excitation fluence. As shown in Fig. 2, we observe distinct behavior for the prompt and slow components fluorescence emission. The amplitude of the slow emission component increases linearly with pump power for

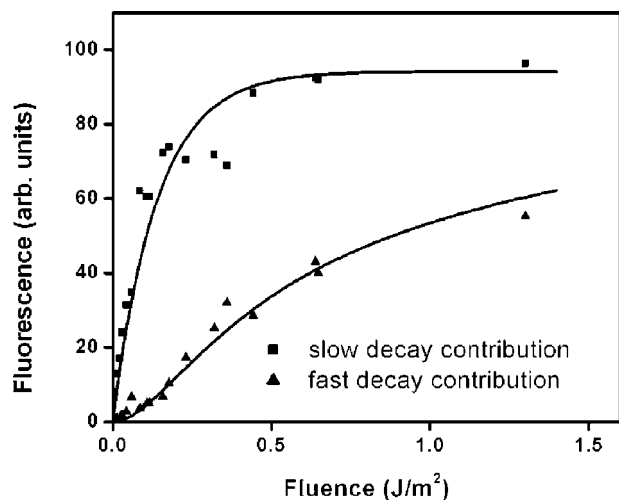


FIG. 2. The dependence of the integrated fluorescence emission in the slow (squares) and the fast (triangles) components as a function of the excitation pump fluence. The curves are fits to the model described in the text.

low excitation levels, but shows strong saturation at fluences above ≥ 0.3 J/m². The fast component, on the other hand, continues to grow with increasing fluence, with only a weak incipient saturation setting in at the highest fluences. As a complementary study, we recorded the transient absorption at the E_{11} band edge of SWNTs following photoexcitation. The main features seen in the time-resolved fluorescence data, including the emergence of a fast decay component and strong saturation of the tail of the decay at high excitation fluence, were reproduced in these measurements. Similar effects were recently reported by Ma *et al.*²²

To understand the nanotube fluorescence dynamics, let us consider possible physical processes that might occur at elevated excitation densities. A common phenomenon at high excitation fluence is absorption saturation. This effect would, however, only change the carrier density and would not alter the temporal evolution of the decay. Furthermore, direct measurement of the absorption as a function of laser fluence shows that the nanotube absorbance at 810 nm remains essentially identical, even for the highest pump fluence used in these studies. This fact also excludes two-photon absorption effects. One may then ask whether the observed dynamics can be attributed to saturation of the trapping states at high excitation density. This scenario is implausible because it would suggest a slower decay rate at high fluences, while we actually see the emergence of a faster decay component in this regime.

A different class of effect involves multiple carrier-carrier interactions. Such processes are well documented not only in bulk materials,⁶⁻⁹ but also in semiconductor nanoparticles¹⁰⁻¹² where Auger recombination may play a dominant role when extra carriers or multiple excitations are present. In view of the strong-carrier confinement in SWNTs, such processes are also likely to be significant in this case. Indeed, the presence of a rapid Auger recombination in the SWNTs allows us, as we show below, to obtain quantitative agreement with the observed dependence of the fluorescence emission on the nanotube excitation density. Before beginning our quantitative analysis, we wish to describe qualitatively how the existence of a rapid Auger process allows us to account for the characteristic features of experimental data. At low excitation fluence with, at most, one electron-hole pair in each excited nanotube, we observe only the slow component of the fluorescence emission. When more than one electron-hole pair is present in a SWNT, the Auger process opens up a nonradiative recombination channel for electron-hole pair recombination. If the Auger process is sufficiently efficient, it will quickly deplete the population of electron-hole pairs, resulting in the rapid fluorescence quenching seen experimentally. The annihilation of the electron-hole pairs comes to a stop when just a single electron-hole pair remains in a nanotube. Thus at all fluences, the fluorescence after this initial period arises exclusively from the one surviving electron-hole pair and yields the same temporal form of the decay curve. Since all nanotubes are excited at sufficiently high fluence, we expect the tail of the fluorescence emission to be precisely the same, both in temporal form and in amplitude, in this regime. As shown in Fig. 1, this is indeed what is seen experimentally for fluences ≥ 0.3 J/m².

To make our discussion more quantitative, we introduce an explicit model of the carrier dynamics that includes Auger interactions. In analogy to the bulk behavior, the carrier dynamics in nanotubes can be formulated in terms of rate equations. Unlike the case of bulk materials, however, one cannot characterize an ensemble of nanotubes by an average carrier density: The quantized character of number of excitations in a given nanotube must be taken into account. One cannot, for example, describe a situation in which one nanotube in ten is excited simply by saying that the average number of electron-hole pairs per nanotube is 0.1. Thus, we introduce a time-dependent probability distribution $\rho^N(t)$ to describe the probability of a nanotube having $N=0,1,2,3,\dots$ electron-hole pairs. The distribution of excitation number in an ensemble of nanotubes can then be shown to obey a master equation

$$\frac{d\rho^N}{dt} = \rho^{N+1}(\gamma_r^{N+1} + \gamma_A^{N+1} + \gamma_t)(N+1) - \rho^N(\gamma_r^N + \gamma_A^N + \gamma_t)N. \quad (1)$$

In this equation, we have included changes in the carrier number associated with radiative emission, Auger recombination, and carrier trapping at defects, characterized, respectively, by rates γ_r^N , γ_A^N , and γ_t . For the radiative and Auger processes, we have explicitly noted their possible dependences on the number N of electron-hole pairs in the nanotube. These dependences will be discussed below. The initial distribution of excitations in the nanotube ensemble is taken to be Poissonian with a mean excitation number of $\sigma\phi$, the product of nanotube absorption cross section at the 810-nm pump wavelength and the number of photons per unit area in a pump pulse. The fluorescence emission rate (per nanotube) as a function of time, $F(t)$, can then be obtained by considering the emission rate from the ensemble of nanotubes,

$$F(t) = \sum_{N=1}^{\infty} (\gamma_r^N \times N \times \rho^N). \quad (2)$$

To proceed further, we must consider the parametric dependence of the radiative (γ_r^N) and Auger (γ_A^N) recombination rates on the number of electron-hole pairs in the nanotube. These relations differ depending on the degree of electron-hole correlation, with distinct behavior for free carriers and excitons. Assuming free motion of the relevant excitations throughout the nanotube, we have for excitons

$$\gamma_r^N = \text{const}, \quad \gamma_A^N \propto (N-1)$$

and for free carriers

$$\gamma_r^N \propto N; \quad \gamma_A^N \propto N(N-1).$$

Note that in this regime of just a few carriers, it is important to distinguish dependences scaling as N from those scaling as $N-1$, a consideration that is not relevant in the bulk limit of large carrier numbers. As for the proper description of the excitations in the SWNTs, a free-carrier picture has been used to describe many of the experimental results.^{2,14} Recent theoretical considerations indicate, however, that excitonic effects are quite significant in SWNTs.²³ Thus we discuss our

observations within the excitonic framework.

Our model for the temporal evolution of the fluorescence is defined by four parameters: The radiative emission rate γ_r , the Auger rate, which for the excitons can be written as $\gamma_A = C_A(N-1)$, the trapping rate γ_t , and the mean initial excitation number $\phi\sigma$. From previous studies,²¹ the radiative emission is shown to be ~ 100 ns and thus far slower than the other rates in the problem. In this case, the rate of radiative emission appears only as an overall scale factor for the emission strength and does not affect the dynamics. Another of the parameters, the trapping rate $\gamma_t (= 1.6 \times 10^{11} \text{ s}^{-1})$ is determined directly from the measured fluorescence decay in the limit of low excitation. Thus, our fit of the dynamics is determined by just two parameters, the Auger rate coefficient C_A and the excitation number $\phi\sigma$. We note further that the photon fluence ϕ is known from experiment, so we can describe the two adjustable parameters as the absorption cross-section σ and the Auger coefficient C_A . These values are determined from the fluence dependence of the fast and slow fluorescence yields shown in Fig. 2. The Auger rate, which we discuss below, is found to be given by $C_A = 0.8 \text{ ps}^{-1}$. With all parameters now fixed, we can apply the model to predict the full temporal evolution of the fluorescence at various excitation densities. For comparison with experiment, we then convolve the prediction with the measured Kerr-gate response function.²¹ The results, shown as the gray curves in Fig. 1, fit not only the fluorescence decay curve for one excitation density, but *the entire set* of decay curves measured over a wide range of pump fluences.

The Auger annihilation lifetime for an exciton is given by $\tau_A^N \equiv (\gamma_A^N)^{-1} = C_A^{-1}(N-1)^{-1}$ for a nanotube with N electron-hole pairs. Using the inferred Auger coefficient of $C_A = 0.8 \text{ ps}^{-1}$ in our typical 380-nm-long SWNTs, we find the Auger annihilation lifetime to be as short as 1.2 ps with just two electron-hole pairs in a nanotube. In the exciton picture, this lifetime scales linearly with the length of nanotubes and the Auger lifetime for two electron-hole pairs in a nanotube of length $L \mu\text{m}$ will be $\sim 3L$ ps. Our experimental findings thus indicate that multiple electron-hole pairs can persist in a micron long nanotube for at most a few picoseconds. To get a feeling of this Auger annihilation lifetime, it is instructive to compare the experimental behavior for the SWNT with what one might expect if Auger recombination were occurring in a bulk material at an equivalent excitation density. Since bulk Auger rates vary strongly with the band gap of the material, we consider a III-V alloy, $\text{In}_{0.78}\text{Ga}_{0.22}\text{As}_{0.5}\text{P}_{0.5}$, with a band gap similar to the nanotube system. The effective bulk density corresponding to two excitons in a nanotube can be taken as $2/(AL)$, where A is the nanotube cross-sectional area and L is its length. The resulting bulk Auger lifetime is then found to be ~ 1000 ps, far longer than that in SWNTs. The strength of the Auger recombination process in SWNTs can be attributed to the enhancement of carrier-carrier interactions in the quasi-1D nanotube system. Our results highlight the need for a full quantum mechanical calculation of the behavior in nanotubes, since the distinctive nanotube structure precludes even a rough estimate of the Auger rate from comparisons with the well-studied bulk materials.

The existence of rapid Auger recombination in SWNTs

sets a stringent limit on the sustained electron-hole pair densities that one may expect to achieve experimentally. This situation is particularly relevant for attempts to achieve population inversion and light amplification in SWNTs. Even for incoherent nanotube light-emitting devices based on electroluminescence, Auger processes may reduce the emission efficiency for high rates of carrier injection or long carrier lifetimes. Although not directly examined in this study, our work suggests that the presence of free electrons or holes in SWNT, arising, for example, from impurities or electric fields, may also induce rapid annihilation of electron-hole pairs through the Auger process. This effect may play a role

in the strong variation of photoluminescence efficiency observed at acidic pH.^{17,24}

The authors wish to acknowledge helpful discussions with M. Hybertsen. Primary support for this work was provided by the Nanoscale Science and Engineering Initiative of the NSF under Grant No. CHE-0117752 and by the New York State Office of Science, Technology, and Academic Research (NYSTAR), and by the Office of Basic Energy Science of the DOE under Grant Nos. FG02-98ER14861 and FG02-03ER15463.

*Permanent address: Department of Physics and Astronomy, Rowan University, 201 Mullica Hill Road, Glassboro, New Jersey 08028.

¹S. Iijima, *Nature (London)* **354**, 56 (1991).

²R. Saito, G. Dresselhaus, and M. S. Dresselhaus, *Physical Properties of Carbon Nanotubes* (Imperial College Press, London, 1998).

³Special Issue on Carbon Nanotubes, edited by R. C. Haddon, *Acc. Chem. Res.* **35**, 997–1113 (2002).

⁴R. Martel, V. Derycke, C. Lavoie, J. Appenzeller, K. K. Chan, J. Tersoff, and P. Avouris, *Phys. Rev. Lett.* **87**, 256805 (2001).

⁵J. A. Misewich, R. Martel, P. Avouris, J. C. Tsang, S. Heinze, and J. Tersoff, *Science* **300**, 783 (2003).

⁶G. P. Agrawal and N. K. Dutta, *Long-Wavelength Semiconductor Lasers* (Van Nostrand Reinhold, New York, 1986).

⁷D. J. Roulston, *Bipolar Semiconductor Devices* (McGraw-Hill, New York, 1990).

⁸M. A. Green, *Silicon Solar Cells: Advanced Principles and Practice* (UNSW, Sydney, 1995).

⁹R. F. Pierret, *Advanced Semiconductor Fundamentals* (Addison-Wesley, Reading, MA, 1989).

¹⁰V. I. Klimov, A. A. Mikhailovsky, D. W. McBranch, C. A. Leatherdale, and M. G. Bawendi, *Science* **287**, 1011 (2000).

¹¹C. Delerue, M. Lannoo, G. Allan, E. Martin, I. Mihalcescu, J.C. Vial, R. Romestain, F. Muller, and A. Biesy, *Phys. Rev. Lett.* **75**, 2228 (1995).

¹²V.I. Klimov, A.A. Mikhailovsky, S. Xu, A. Malko, J.A. Hollingsworth, C.A. Leatherdale, H.-J. Eisler, and M.G. Bawendi,

Science **290**, 314 (2000).

¹³J.S. Lauret, C. Voisin, G. Cassabois, C. Delalande, P. Roussignol, O. Jost, and L. Capes, *Phys. Rev. Lett.* **90**, 057404 (2003).

¹⁴A. Hagen, G. Moos, V. Talalaev, and T. Hertel, *Appl. Phys. A: Mater. Sci. Process.* **78**, 1137 (2004).

¹⁵O. J. Korovyanko, C. X. Sheng, Z. V. Vardeny, A. B. Dalton, and R. H. Baughman, *Phys. Rev. Lett.* **92**, 017403 (2004).

¹⁶G.N. Ostojic, S. Zaric, J. Kono, M.S. Strano, V.C. Moore, R.H. Hauge, and R.E. Smalley, *Phys. Rev. Lett.* **92**, 117402 (2004).

¹⁷M.J. O'Connell, S.M. Bachilo, C.B. Huffman, V.C. Moore, M.S. Strano, E.H. Haroz, K.L. Rialon, P.J. Boul, W.H. Noon, C. Kittrell, J. Ma, R.H. Hauge, R.B. Weisman, and R.E. Smalley, *Science* **297**, 593 (2002).

¹⁸Purchased from Carbon Nanotechnologies, Inc. (Houston, TX).

¹⁹P. P. Ho and R. R. Alfano, *Phys. Rev. A* **20**, 2170 (1979).

²⁰J. Takeda, K. Nakajima, S. Kurita, S. Tomimoto, S. Saito, and T. Suemoto, *Phys. Rev. B* **62**, 10083 (2000).

²¹F. Wang, G. Dukovic, L. E. Brus, and T. F. Heinz, *Phys. Rev. Lett.* **92**, 177401 (2004).

²²Y.Z. Ma, J. Stenger, J. Zimmermann, S.M. Bachilo, R.E. Smalley, R.B. Weisman, and G.R. Fleming, *J. Chem. Phys.* **120**, 3368 (2004).

²³V. Perebeinos, J. Tersoff, and P. Avouris, *Phys. Rev. Lett.* **92**, 257402 (2004) and references therein.

²⁴G. Dukovic, B. E. White, Z. Y. Zhou, F. Wang, S. Jockusch, M. Steigerwald, T. F. Heinz, R. A. Friesner, N. J. Turro, and L. E. Brus, *J. Am. Chem. Soc.* **126**, 15 269 (2004).